Molecular Vision 2005; 11:729-37 <http://www.molvis.org/molvis/v11/a86/>
Received 27 May 2005 | Accepted 3 August 2005 | Published 12 September 2005

©2005 Molecular Vision

Cancer stem cell characteristics in retinoblastoma

Gail M. Seigel,[1,2] Lorrie M. Campbell,[1,2] Malathi Narayan,[1,2,4] Federico Gonzalez-Fernandez[1,2,3,4]

[1]Ross Eye Institute and the Departments of [2]Ophthalmology and [3]Pathology, University of Buffalo, Buffalo, NY; [4]Medical Research Service, Veterans Affairs, Buffalo, NY

Purpose: There is increasing evidence that cancer stem cells contribute to tumor progression and chemoresistance in a variety of malignancies, including brain tumors, leukemias, and breast carcinomas. In this study, we tested the hypothesis that retinoblastomas contain subpopulations of cells that exhibit cancer stem cell properties.
Methods: The following sources of retinoblastoma cells andtissues were examined for the presence of stem cell markers by immunocytochemistry: retinoblastoma tumors from mice transgenic for the SV40 T-antigen (driven by the β-luteinizing hormone promoter), cell pellets of human Y79 and WERI-Rb27 retinoblastoma cell lines, and archival human retinoblastoma pathological specimens. Hoechst dye exclusion, mediated by the stem cell surface marker ABCG2 (ATP-binding cassette transporter, G2 subfamily), was assessed by flow cytometry in mouse tumors and WERI-Rb27 cells.
Results: Small numbers of retinoblastoma cells (less than 1%) exhibited immunoreactivity to stem cell markers ABCG2, aldehyde dehydrogenase 1 (ALDH1), MCM2 (minichromosome maintenance marker 2), SCA-1 (Stem cell antigen-1), and p63. Hoechst dye uptake in mouse tumors and WERI-Rb27 cells was enhanced by addition of 50 μM Verapamil, consistent with activity of the calcium-sensitive ABCG2 protein. Flow cytometric analysis confirmed the presence of small subpopulations of cells excluding Hoechst dye in mouse retinoblastoma tumors (0.3%) and WERI-Rb27 cells (0.1%) in a verapamil-sensitive manner. ABCG2 and ALDH1 positive cells were Hoechst-dim, as seen by dual labeling in vitro.
Conclusions: Mouse and human retinoblastoma tumor cells contain a small subpopulation of cells that exhibit a cancer stem cell-like phenotype. Especially significant is the expression of ABCG2 in mouse and human tumor cells, a calcium-sensitive cell surface protein that not only acts to exclude Hoechst dye, but also confers resistance to over 20 different chemotherapeutic agents. These findings point to a heterogeneity in retinoblastoma tumors that may have significant impact on future treatment strategies.

Retinoblastomas arise when both alleles of the *rb* gene are inactivated in the same retinoblast. *Rb* codes for a nuclear phosphoprotein that regulates retinoblast proliferation and development [1]. As proposed more than two decades ago, retinoblastoma arises from a primitive neuroectodermal cell [2]. The malignant cells typically express a restricted set of markers, particularly IRBP and cone-specific genes, and form various rosette structures representing photoreceptor differentiation. This expression pattern follows the cone photoreceptor default pathway of retinal development. Thus, although the target cell is a pluripotent retinoblast, the cellular phenotype largely resembles that of photoreceptors, in which cones are the dominant cellular phenotype [3,4]. For many years, an elusive goal has been to identify the retinoblastoma cell of origin [5]. There has been a general consensus in the literature that primitive neuro-ectodermal cells are in some way involved in RB tumorigenesis [6,7]. More recently, the theory of a "cancer stem cell" component to retinoblastoma has been put forward [5].

Correspondence to: Gail M. Seigel, Ross Eye Institute, Department of Ophthalmology, University of Buffalo, 3435 Main Street, Sherman 124, Buffalo, NY, 14214; Phone: (716) 829-2157; FAX: (716) 829-2157; email: gseigel@frontiernet.net

Dr. Malathi Narayan is now a graduate student in the Department of Biochemistry, Medical College of Wisconsin, Madison, WI

The hypothesis of cancer "stem cells" originates from previous observations that not every cell within a tumor can maintain tumor growth, and that large numbers of tumor cells are needed to transplant a tumor. Some cancers appear to contain stem-like cells (cancer stem cells) that are slowly dividing, chemoresistant, and are capable of tumor progression [8,9]. The existence of cancer stem cells was first shown in acute myeloid leukemia [10,11] and has since been demonstrated in other cancers, including breast cancer [12] human brain tumors [13] and even the C6 glioma cell line, maintained in culture over many years [14]. Therefore, there is precedent for the persistence of cancer stem cells with unique stem cell-like properties. Yet, we still do not know whether all cancers are organized into a hierarchy of cells with different proliferative and differentiation potentials.

ABCG2 (or BCRP), an ATP-binding cassette transporter in the G2 subfamily, is a cell surface, drug-resistance marker that has been utilized to identify stem cells from a variety of tissues, including tumors and leukemias. Specifically, ABCG2 expression confers upon cells the ability to exclude Hoechst dye 33342 [15-17], and confer resistance to at least 20 different chemotherapeutic agents, including methotrexate, doxorubicin, indolcarbazole, and others [18]. This dye-excluding "side population" (SP) phenotype has been used in a variety of tissues to sort out presumptive stem cells, including stem cells from hematopoetic populations [16], bone marrow, skeletal muscle [17], mammary gland [19], lung [20], and devel-

oping retina [21]. The side population has been identified as a group of cells able to exclude the Hoechst 33342 dye, a characteristic abolished with 50 μM verapamil treatment [22]. The SP phenotype, coupled with expression of stem cell markers are two of the hallmarks of stem cells, both cancer stem cells and otherwise. In the present study, we tested the hypothesis that retinoblastoma contains subpopulations of cells that express these unique stem cell characteristics.

METHODS

Animals: Animal experiments were performed in accordance with NIH guidelines (DHEW publication NIH80-23) and with approval by the Institutional Animal Care and Use Committee of the Veterans Affairs Medical Research Service. Fresh retinoblastoma (RB) tumors were harvested from adult SV40 β-LH-T-Ag mice. Breeding pairs of mice for the initiation of our colony were generously provided by Dr. Daniel Albert [23]. The mouse model was created by expression of a viral oncogene (simian virus 40 T-Antigen), in the retina of transgenic mice, resulting in heritable ocular tumors with histological, ultrastructural and immunohistochemical characteristics comparable to those of human RB [23]. Animals were killed by CO_2 inhalation and their eyes placed in 4% paraformaldehyde buffered with PBS. The fixed eyes were incubated in 30% sucrose and OCT compound. Frozen sections were cut for immunohistochemistry.

Cells: For cell culture studies, we used the well-established cell lines Y79 [24] and WERI-Rb27 [25], derived from genetically related donors [26]. The WERI-Rb27 cell line was derived from a 24-month-old boy with bilateral retinoblastoma, with abnormal mRNA transcripts corresponding to the retinoblastoma gene. Y79 cells originated from the intraocular tumor of a 2 1/2 year-old female. WERI-Rb27 cells were maintained in DMEM with 10% calf serum, 1X MEM nonessential amino acids (GIBCO, Grand Island, NY), 1X MEM vitamins (GIBCO), 0.37% sodium bicarbonate, 0.058% l-glutamine and 100 μg/ml gentamicin. Y79 cells were maintained in RPMI 1640 with 20% fetal calf serum, 0.37% sodium bicarbonate, 0.058% l-glutamine, 10 mM HEPES, and 100 μg/ml gentamicin.

Human archival RB tumor specimens: Serial paraffin sections of three human RB tumors were examined for the presence of stem cell markers. Three human RB cases were used for comparison with the human cell lines and mouse tumors. However, three human cases were insufficient to make statistically significant correlations between expression of stem cell markers and tumor stage, treatment or prognosis. This will be the topic of a future study.

Table 1. Primary antibodies

Antibody	Company (catalog number)	Concentration
ABCG2	Signet Labs (BXP-21)	6.25 μg/ml
ALDH1	Transduction Labs (A84320)	2.5 μg/ml
SCA-1	BD Biosciences (E13.161.7)	5 μg/ml
MCM2	Santa Cruz Biochem (N-19)	2 μg/ml
p63	BD Biosciences (55951)	5 μg/ml

This is a listing of the primary antibodies used for immunocytochemistry, along with commercial sources and working concentrations for staining.

Immunohistochemistry: Table 1 lists the primary antibodies, their sources, and concentrations for all staining techniques used in this report. For negative controls, we tested these antibodies on mouse fibroblasts (NIH 3T3 cells) and human cervical carcinoma cells (HeLa cells), with no staining observed (data not shown). Paraffin-embedded retinal tissue sections of archival human specimens were rehydrated through xylene and graded alcohols and underwent antigen retrieval. Antigen retrieval was accomplished by placing slides in 10 mM sodium citrate buffer (pH 6.0), heated at 95 °C for 10 min. The slides and buffer were then cooled to room temperature over an interval of 20 min, followed by three rinses in water for 2 min each. The water was blotted off and the primary antibody was added to the slides. Frozen sections skipped the previous steps and were rinsed directly in PBS, then carried through the rest of the protocol. Goat serum (5%) was used for blocking of nonspecific staining on slides. All tissue sections were incubated in 0.25% Triton X-100 for 5 min. After a rinse in phosphate-buffered saline (PBS), sections were incubated for 1 h with primary antibody. After rinsing three times for 5 min each in PBS, sections were incubated with 1 μg/ml of biotinylated goat anti-rabbit or anti-mouse immunoglobulin (Zymed/Invitrogen, Carlsbad, CA) for 60 min. Tissue sections were incubated for 20 min with horseradish peroxidase-conjugated avidin (Elite kit, Vector Laboratories, Burlingame, CA). The sections were rinsed in 0.05 M Tris (pH 7.4) and antigens were detected with diaminobenzidine (Vector). The brown to black reaction product was visualized by light microscopy. Negative controls that consisted of incubations in 5% isotype control serum without primary antibody did not generate reaction product.

Fluorescent immunostaining in suspension: WERI-Rb27 cells and dissociated mouse tumor cells were double labeled in suspension with Hoechst 33342 and either ABCG2 or ALDH1. Cells ($2x10^6$) were centrifuged at 800 rpm (149x g) for 5 min. The supernatant was decanted and cells resuspended in 4 ml of DMEM with 10% calf serum. Hoechst 33342 dye (Molecular Probes, Eugene, OR) was added at 5 μg/ml, and cells were incubated at 37 °C for 90 min. Cells were washed twice in PBS and centriguged at 149x g for 5 min. Cells were resuspended in 200 μl PBS and divided into two tubes. No blocking serum was used. One tube received 6.25 μg/ml ABCG2 antibody and was incubated 1 h at room temperature, while the other tube received 5% isotype control antibody. Cells were washed two times with PBS and resuspended in 100 μl PBS. TRITC conjugated anti-mouse IgG (Sigma Chemical, St. Louis, MO) was added at 1:100 dilution to both tubes. Cells were incubated for 1 h at room temperature. Cells were washed two times with PBS and resuspended in residual supernatant after decanting, then pipetted onto a slide and coverslipped for microscopic viewing. Fluorescent cells were visualized with a Nikon ES600 microscope with epifluorescent filters for Hoechst and TRITC. Images were captured with a

SONY ICX 285AL SPOT camera (Diagnostic Instruments, Sterling Heights, MI).

Identification of side populations: Methods for identification of side populations were adapted from previous reports [26,27]. Briefly, cells were incubated with 5 μg/ml Hoechst 33342 dye (with or without verapamil (MP Biomedicals, Eschwege, Germany)) for 90 min, rinsed in PBS and centrifuged at 149x g for 5 min. Cells were resuspended in PBS with 2 μg/ml propidium iodide (Sigma). Cell samples (mouse tumor cells and WERI-Rb27 cells) were analyzed at the Roswell Park UV cell sorter facility using a FACSVantage cell sorter with Turbosort with UV capabilities and CellQuest software for data acquisition and analysis. An Argon laser (333-363 nm) was used to excite the Hoechst dye. Fluorescence emission was collected with a 405/30 nm band pass filter for Hoechst blue and a 660 nm ALP (long pass filter) for Hoechst red. Dead cells were excluded by propidium iodide fluorescence at 564-606 nm. The side population "SP" was identified as a group of cells able to exclude the Hoechst dye, a characteristic abolished with 50 μM verapamil treatment [22].

RESULTS

RB side populations (SPs) detected by flow cytometry: In previous studies, using a novel microtiter assay, we have shown verapamil-sensitive Hoechst 33342 dye uptake in WERI-Rb27 cells, Y79 cells, and mouse tumor cells, but not NIH 3T3 mouse fibroblast cells [28]. In this study, we examined cells from mouse tumors, and WERI-Rb27 cells for the presence of side populations by flow cytometry. As seen in Figure 1, a small, but persistent number of cells (0.3% for the mouse tumor, 0.1% for WERI-Rb27) displayed uptake of Hoechst 3342 dye that was abolished by the addition of 50 μM verapamil, the definition of a side population [22]. As seen in Figure 1, boxes are drawn that bound the area of the side population.

ABCG2 staining co-localizes with Hoechst-dim cells in RB: The presence of side populations in RB cell cultures, as seen in Figure 1, led us to examine the co-localization of Hoechst-dim cells with ABCG2 immunoreactive cells in SV40 β-LH-T-Ag mouse tumors, WERI-Rb27, and Y79 cells. If, in fact, ABCG2 confers the ability to exclude Hoechst dye, one would predict that cells immunoreactive for ABCG2 would necessarily be Hoechst-dim. This result is shown in Figure 2. In each case, cells that were ABCG2 bright (less than 1% of the population, Figure 2A,E,I), were Hoechst-dim (Figure 2B,F,J), as seen definitively in the merged image (Figure 2C,G,K). Brightfield images were captured (Figure 2D,H,L) to ensure that the labeled cells appeared healthy and intact. It was important to determine cell morphology, as less intact cells

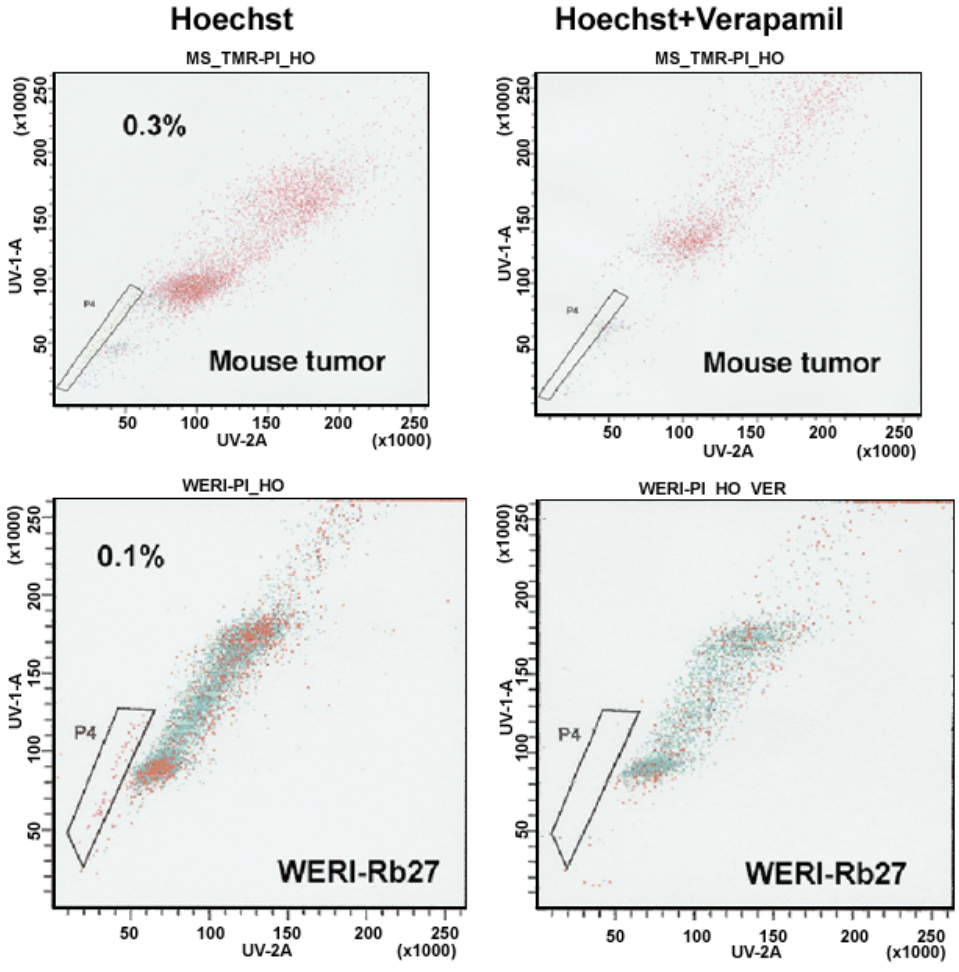

Figure 1. RB side populations (SPs) detected by flow cytometry. Side populations, characteristic of a stem cell phenotype, are identified by verapamil-sensitive exclusion of the Hoechst 33342 fluorescent dye. In this experiment, cell suspensions were incubated with Hoechst 33342 dye and analyzed by flow cytometry as described in Methods. Cancer stem cells would be expected to exclude the dye, except in the presence of verapamil, a drug that can abolish the dye excluding properties of the ABCG2 transporter. The fluorescence intensities of each cell in a population of at least 10,000 are plotted (Hoechst blue [y-axis] versus Hoechst red [x-axis]). The axes represent fluorescence intensities. The side population region was defined on the basis of fluorescence emission in both red and blue wavelengths. Boxes were drawn (labeled P4) to indicate verapamil-sensitive, Hoechst-excluding side populations. Both WERI-Rb27 and fresh SV40 βLH-T-Ag mouse RB tumors were found to contain side populations, and the percentage of cells in the boxes (as a percentage of the total number of live cells) is given in each plot. Cells within these P4 boxes are putative cancer stem cells.

occasionally took up the TRITC-conjugated secondary antibody in a nonspecific manner.

ALDH1 staining co-localizes with Hoechst-dim cells in RB: Aldehyde dehydrogenases (ALDHs) are intracellular enzymes that oxidize aldehydes to carboxylic acids [29]. Measures of ALDH1 activity have been used successfully to enrich for hematopoetic progenitor populations [30]. We stained WERI-Rb27 and Y79 cells to detect the presence of ALDH1-immunopositive/Hoechst dim cells that would further indicate a potential cancer stem cell phenotype. In each case, cells that were ALDH1 bright (less than 1% of the population, Figure 3A,E), were Hoechst-dim (Figure 3B,F), as seen more definitively in the merged image (Figure 3C,G). Brightfield images were captured (Figure 3D,H) to ensure that the labeled cells appeared healthy and intact.

Subpopulations of mouse RB cells are immunoreactive to stem cell markers: We examined immunoreactivity of stem cell and progenitor markers in frozen sections of SV40 βLH-T-Ag mouse tumors (Figure 4). A negative control panel (isotype control serum) is shown in Figure 4A. Stem cell/progenitor cell markers were detected immunohistochemically in small numbers of mouse RB tumor cells (less than 1%). These markers included: ALDH1 (Aldehyde dehydrogenase-1, Figure 4B), SCA-1 (mouse-specific stem cell antigen, Figure 4C) [19], the chemoresistance marker ABCG2 (Figure 4D), and p63 (Figure 4E), a marker expressed by corneal limbal epithelial stem cells [31]. It is important to note that there are six known isoforms of p63 with distinct subcellular localization patterns (nuclear versus cytoplasmic) and different antibody specificities. The particular antibody that we used from BD Biosciences is clone 4A4, a mouse IgG2A made against the N-terminal portion (amino acids 1-65) of a p63-GST fusion protein that cross reacts with both human and mouse p63. This antibody detects both nuclear and cytoplasmic portions of the protein. In all cases, these markers were observed in frozen sections of mouse RB tumors, with less than 1% of the cells immunoreactive.

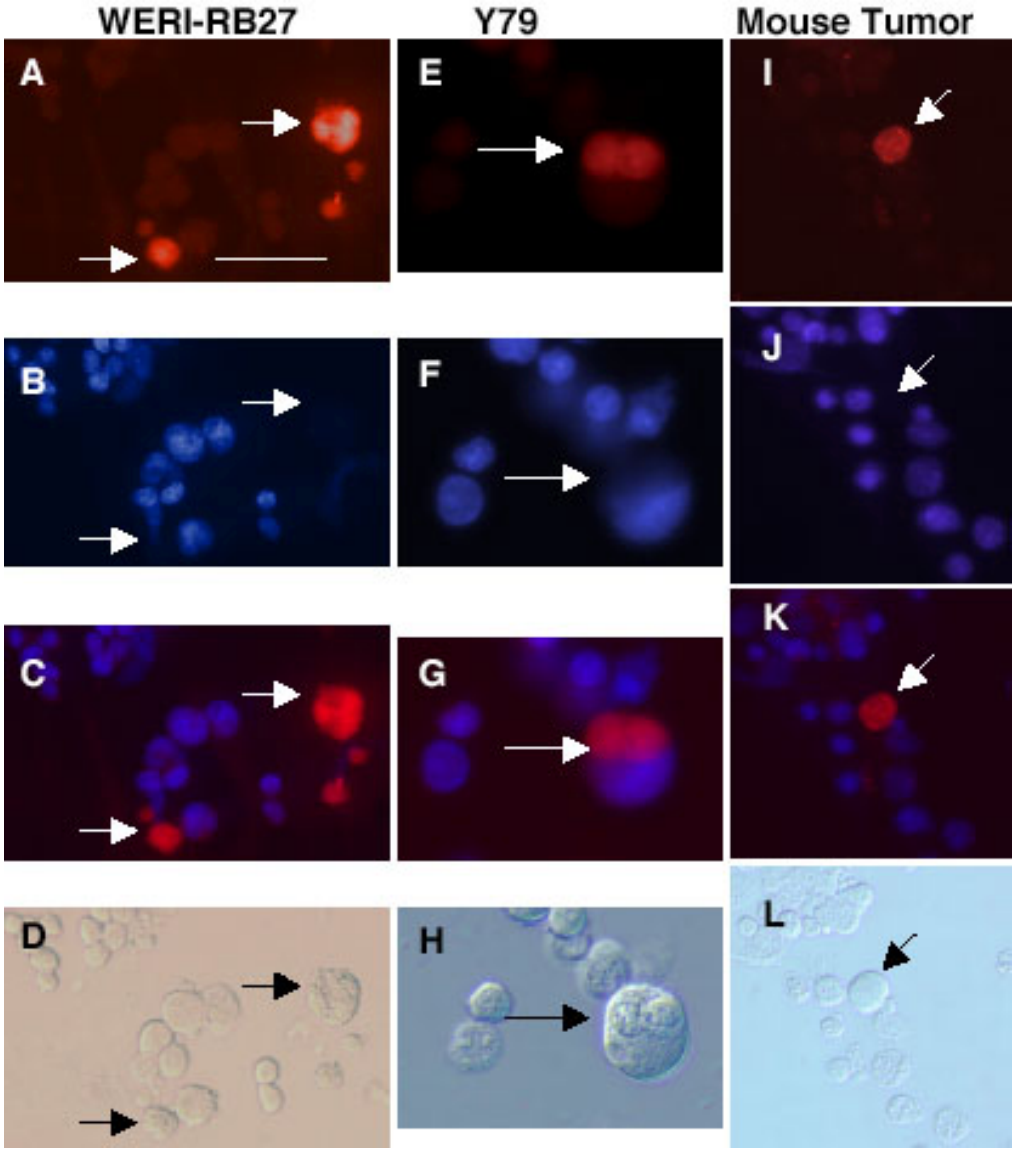

Figure 2. Co-localization of ABCG2 staining with Hoechst-dim cells in human and mouse RB. For each cell type, we examined ABCG2 immunoreactivity along with Hoechst dye uptake in a dual-labeling experiment. Stem cells that reside in a side population are typically ABCG2-bright and Hoechst-dim. The left column (**A**-**D**) illustrates the same field of WERI-Rb27 cells. The middle column (**E**-**H**) illustrates the same field of Y79 cells. The right column (**I**-**L**) shows the same field of mouse RB tumor cells. **A**,**E**,**I**: ABCG2 immumnoreactivity (red). **B**,**F**,**J**: Hoechst dye uptake (blue). **C**,**G**,**K**: A merged image (red and blue) of the top two rows. **D**,**H**,**L**: Brightfield images. Arrows point to bright red cells that are immunoreactive for ABCG2 and Hoechst-dim, characteristic of cancer stem cells. Scale bars represent 10 μm.

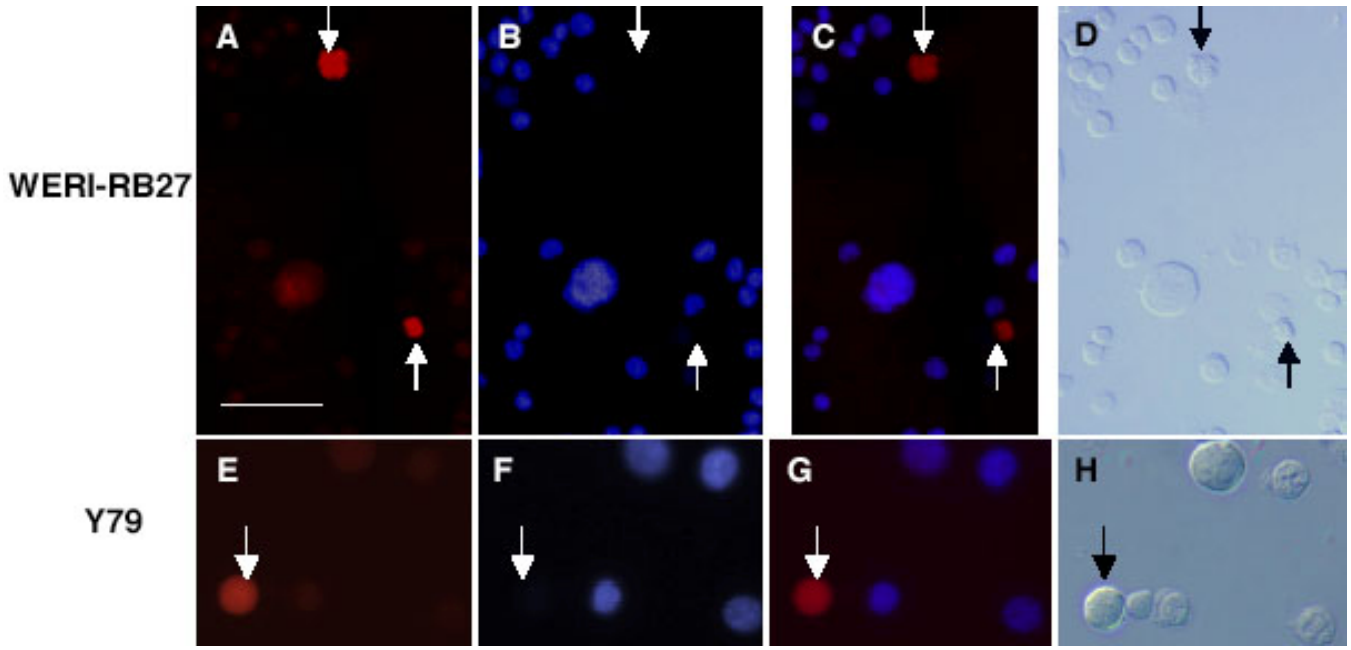

Figure 3. Co-localization of ALDH1 staining with Hoechst-dim cells in RB. For each cell type, we examined ALDH1 immunoreactivity along with Hoechst dye uptake in a dual-labeling experiment. Cancer stem cells would most likely be ALDH1-bright and Hoechst-dim. The top row (**A**-**D**) illustrates the same field of WERI-Rb27 cells. The bottom row (**E**-**H**) illustrates the same field of Y79 cells. **A**,**E**: ALDH1 immunoreactivity is shown in red. **B**,**F**: Hoechst dye uptake is shown in blue. **C**,**G**: Merged images of ALDH1 immunoreactivity and Hoechst dye uptake in WERI-Rb27 cells and Y79 cell line. **D**,**H**: Brightfield images. Arrows point to putative cancer stem cells that are immunoreactive for ALDH1 and Hoechst-dim. Scale bars represent 10 μm.

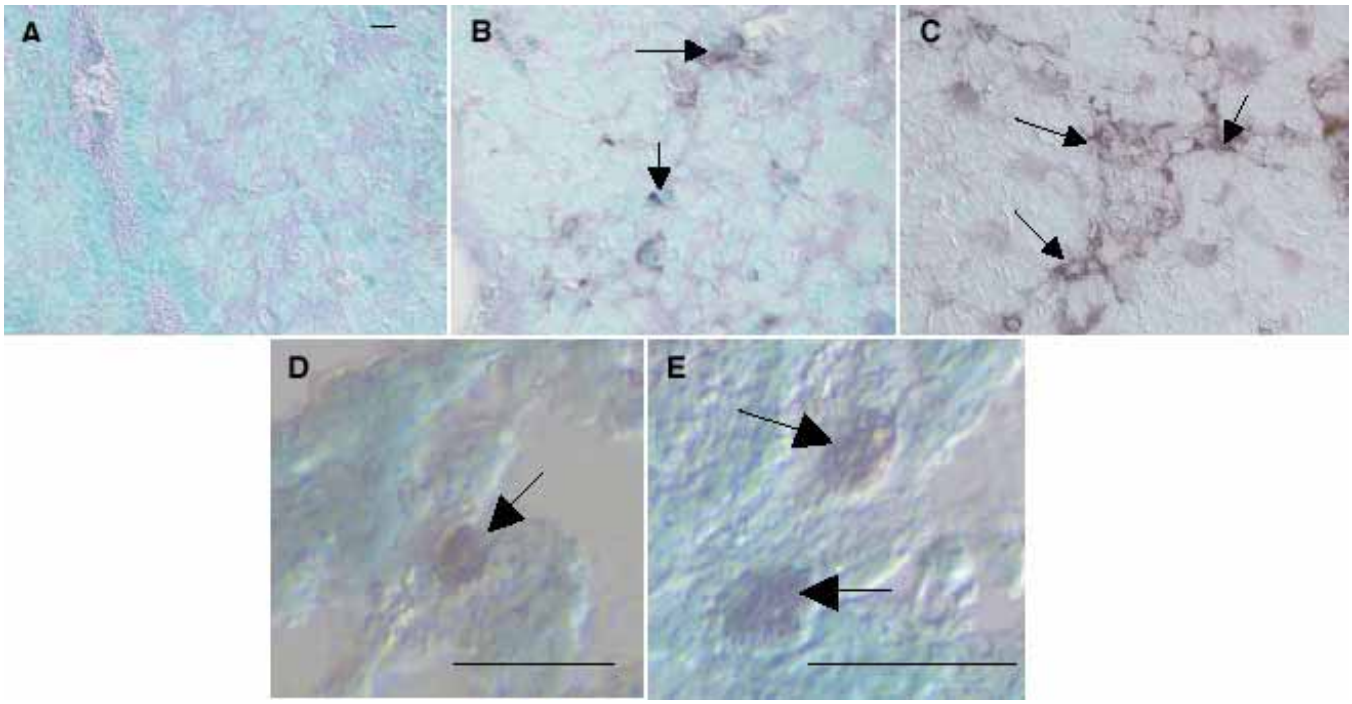

Figure 4. Subpopulations of SV40 βLH-T-Ag mouse tumor cells immunoreactive to stem cell markers. Immunoreactivities of stem cell and progenitor markers were determined in frozen sections of SV40 βLH-T-Ag mouse tumors. Stem cell/progenitor cell markers were detected immunohistochemically in small numbers (less than 1%) of tumor cells. **A**: Negative control panel (goat serum instead of primary antibody). **B**: ALDH1 (Aldehyde dehydrogenase-1). **C**: SCA-1 (mouse-specific stem cell antigen). **D**: Stem cell/chemoresistance marker ABCG2. **E**: p63 (a marker of corneal limbal epithelial stem cells [31]). Scale bars represent 10 μm.

Subpopulations of cells in human RB tissues are immunoreactive to stem cell markers: We examined immunoreactivity of stem cell and progenitor markers in archival human retinoblastoma specimens (Figure 5). These markers included the stem cell/chemoresistance marker ABCG2 (Figure 5A,B) and ALDH1 (Aldehyde dehydrogenase-1, Figure 5C). Interestingly, ABCG2 immunoreactive cells were seen sporadically in the retina (Figure 5B). In both cases, the number of immunoreactive cells was less than 1% of the total number of cells.

Expression of MCM2 in RB: MCM2 (minichromosome maintenance protein 2) exhibits G1 phase-specific expression and is a useful marker for detecting slowly cycling putative neural stem cells in situ [32]. MCM2 is correlated with poor prognosis in lung carcinoma [33]. We examined archival specimens of human RB and detected an interesting pattern of MCM2 expression (Figure 6). MCM2 immunoreactive cells were seen in tumor tissues surrounding blood vessels (Figure 6A), adjacent to the optic nerve (Figure 6B), and sporadically within the retina itself, both in the inner nuclear layer and photoreceptor layer (Figure 6C-E).

DISCUSSION

One present challenge in the treatment of retinoblastoma is the incidence of metastatic or secondary tumors that reduce life span and quality of survival. Patients with germline retinoblastoma have a markedly increased frequency of secondary malignant neoplasms [34]. Those who survive are at increased risk for developing additional malignancies at a rate of about 2% per year [35]. Additional malignancies that occur after primary RB are believed to result from the *Rb* mutation itself, radiation-induced neoplasms, or seeding and invasion of metastatic tumor cells. We propose yet another possible, nonmutually exclusive, mechanism: The persistence of subpopulations of RB cancer stem cells that escape chemotherapy could cause metastasis. As evidence, we present a small subpopulation of RB cells that exhibit some characteristics of a cancer stem cell phenotype including the ABCG2 chemoresistance marker.

We found that expression of MCM2, a neural stem cell marker, is evident not only within the RB tumor itself, but sporadically within histologically unaffected areas of the retina in RB patients. Tumorigenic cells with characteristics similar to neural stem cells have been isolated from pediatric brain tumors [36]. These cells were multipotent, self-renewing and able to produce proliferating neurospheres with the capacity to differentiate into neurons and glia. In a separate study [13], a cell derived from human brain tumors expressed the surface marker ABCG2, self-renewed, and could differentiate in culture to form tumor cells that resembled the original tumor. In addition, there was a positive correlation between self-renewal capacity and increasing aggressiveness of the original tumor. This may explain the poor prognosis of patients having MCM2 immunoreactivity in lung carcinomas [33], and MCM2 could be a similarly important clinical marker in RB, as well. Tumors containing a higher percentage of cancer stem cells may metastasize and spread more readily. As evidence for cell hierarchy within solid tumors, Al-Hajj et al. [12] injected human breast cancer cells into mice and identified a distinct sub-

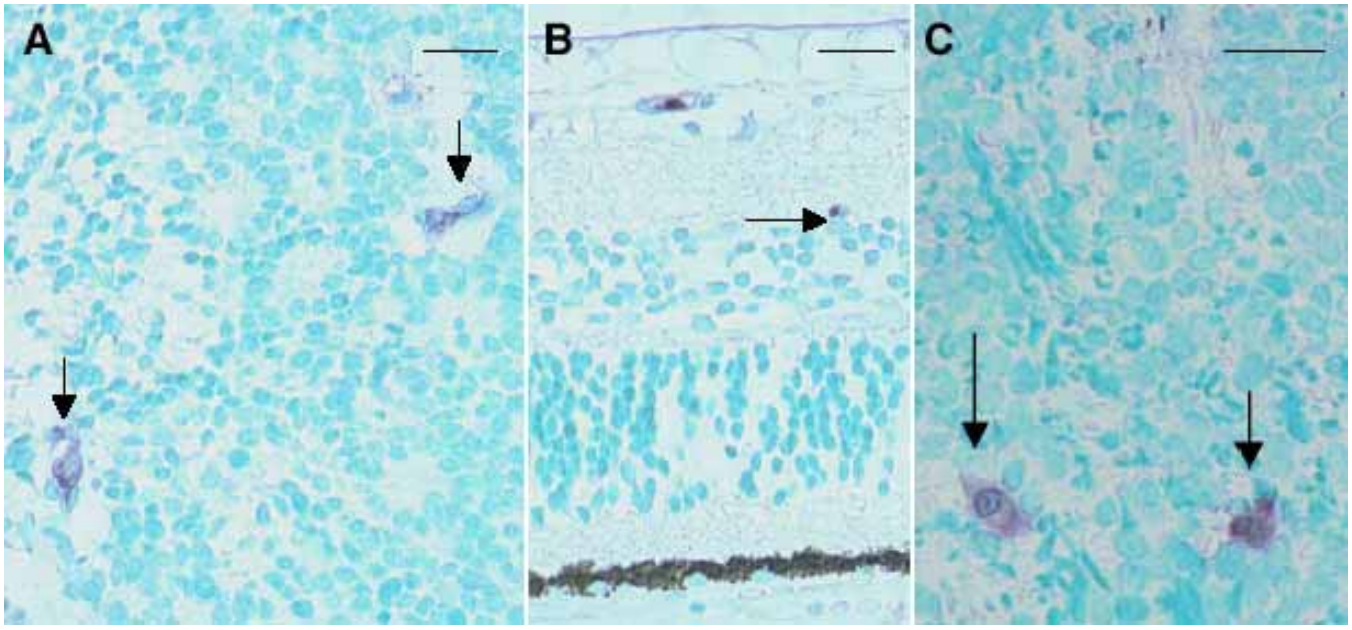

Figure 5. Subpopulations in human RB tissues immunoreactive to stem cell markers. We examined immunoreactivities of stem cell markers ABCG2 and ALDH1 in archival human retinoblastoma specimens. The chemoresistance marker ABCG2 was seen in areas of RB tumor (**A**) and sporadically within the retina itself (**B**). ALDH1 (Aldehyde dehydrogenase-1) immunoreactive human RB tumor cells are shown in (**C**). Immunoreactivity for both ABCG2 and ALDH1 in human tumors suggest the presence of cells that have a stem cell phenotype. Scale bars represent 10 μm.

population capable of generating heterogeneous primary and secondary tumors similar to the original pathology specimens. Their results suggested that the tumorigenic cells can both self-renew and form nontumorigenic cancer cells [12].

Despite the many years since they were first propagated in culture, Y79 and WERI-Rb27 cells appear to have retained their heterogeneity, with regard to cancer stem cell characteristics. As precedent, Kondo et al. [14] analyzed the regenerative and tumor formation potential of six well-known cell lines: C6 (rat glioma), MCF-7 (breast cancer), U-20 and SaOS-2 (osteosarcoma), B104 (rat neuroblastoma), and HeLa (adenocarcinoma, cultured over 50 years). They found that all but the U-20 and SaOS-2 cells contained side population cells. In the C6 glioma line, sorted SP cells could produce both new SP and non-SP cells in culture, produce neurons and glia in culture, and form tumors containing both glia and neurons, when injected into nude mice [14]. It is unknown how long-term propagation may affect RB heterogeneity. Therefore, we included fresh RB mouse tumors, along with preserved human pathological specimens in our analysis.

In summary, mouse and human RB tumor cells contain a small subpopulation of cells that exhibit some cancer stem cell characteristics. Especially significant is the expression of ABCG2, a calcium-sensitive cell surface protein that not only acts to exclude Hoechst dye, but also confers resistance to over 20 different chemotherapeutic agents. Previous studies showed heterogeneous drug resistance marker immunoreactivity in pathology specimens of retinoblastoma, namely the multidrug resistance proteins (MDR)-P-glycoprotein (P-gp) and vault protein lung resistance protein (LRP) [37]. The pres-

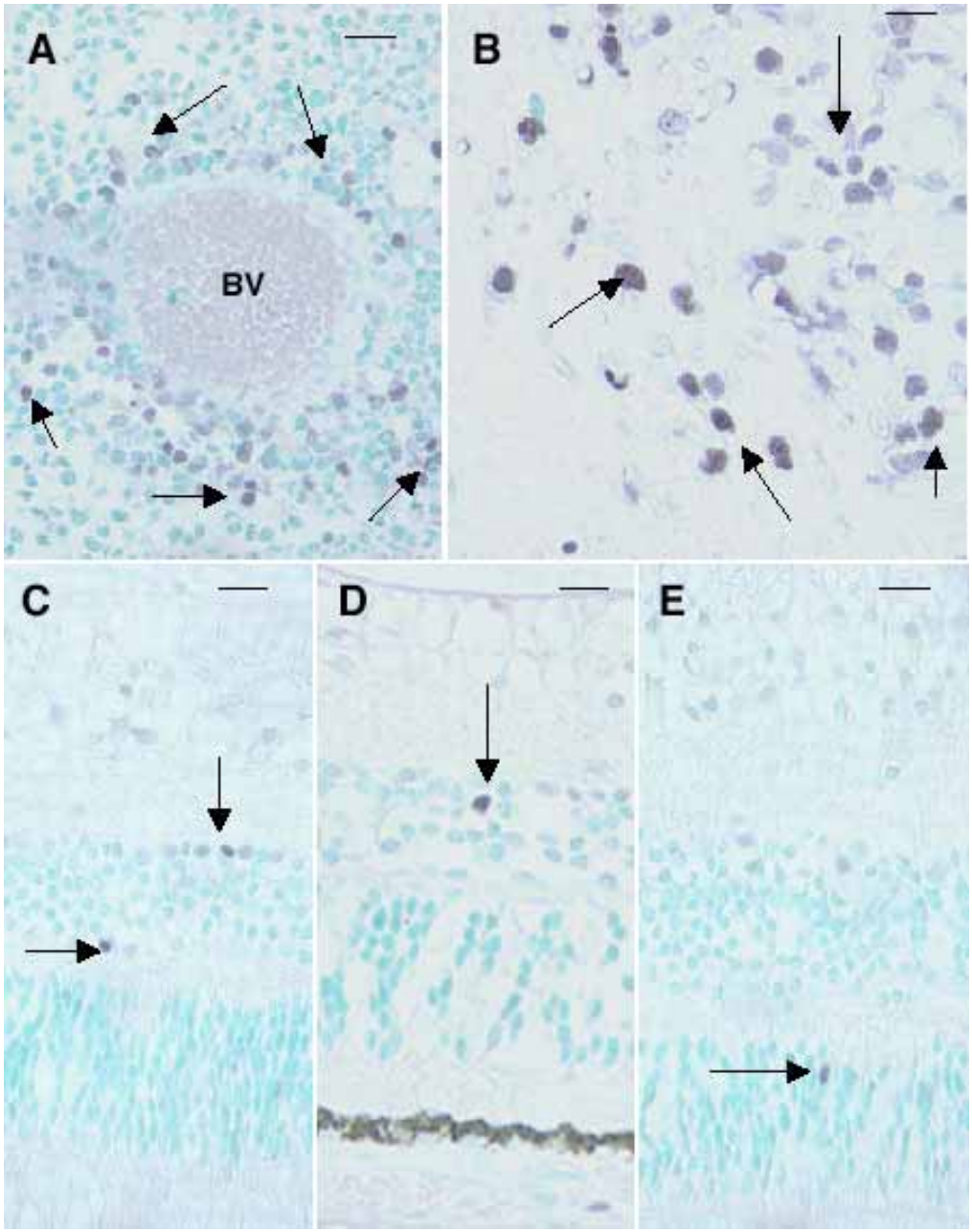

Figure 6. MCM2 immunoreactivity in human RB tissues and retina. MCM2 was localized by immunoreactivity in human retinoblastoma specimens. Positive nuclear staining was evident in tumor cells that are around blood vessels (BV; **A**) and those in solid regions (**B**). Immunoreactive nuclei were found sporadically within the retina in the inner nuclear layer (**C**,**D**) and the photoreceptor layer (**E**). Scale bars represent 10 μm.

ence of these resistance markers, including now ABCG2, suggests the possibility of subpopulations of RB cells that can escape standard chemotherapeutic treatments. In this study, we describe specific stem cell characteristics in retinoblastoma, but we cannot yet assert that these are conclusively cancer stem cells. More studies are needed. Self-renewal experiments, using sorted cells, could be used to show that the isolated side population can eventually generate a population that resembles the original unsorted population. In addition, we are in the process of determining resistance to a panel of chemotherapy drugs, another hallmark of cancer stem cells. Future studies involving transplantation of sorted cells (with and without chemotherapy treatments) will address the issue of metastatic potential.

Major challenges have to be overcome before our understanding of cancer stem cells can be harnessed and translated to meaningful treatments for patients. These challenges include identifying the stem cell subpopulation, characterizing differentiation and tumor-forming potential, and deciding the best therapeutic strategy based upon these findings. The existence of even a small subpopulation of chemoresistant cancer stem cells in retinoblastoma would have a significant impact on therapeutic strategies necessary for tumor eradication.

ACKNOWLEDGEMENTS

The authors thank: David Sheedy of Roswell Park Cancer Institute for technical assistance; Dr. Daniel M. Albert for providing breeding pairs of the SV40 βLH-T-Ag mice. This work was supported by Fight for Sight (GMS) and NEI R01EY009412 (FGF), and an unrestricted departmental grant from Research to Prevent Blindness. Dr. Seigel is also supported by the Sybil Harrington Special Scholar Award from Research to Prevent Blindness. Dr. Gonzalez-Fernandez is the Elizabeth and Ira P. Ross Chair of Ophthalmic Pathology.

REFERENCES

1. Zhang J, Gray J, Wu L, Leone G, Rowan S, Cepko CL, Zhu X, Craft CM, Dyer MA. Rb regulates proliferation and rod photoreceptor development in the mouse retina. Nat Genet 2004; 36:351-60.
2. Kyritsis AP, Tsokos M, Triche TJ, Chader GJ. Retinoblastoma—origin from a primitive neuroectodermal cell? Nature 1984; 307:471-3.
3. Bernstein SL, Kutty G, Wiggert B, Albert DM, Nickerson JM. Expression of retina-specific genes by mouse retinoblastoma cells. Invest Ophthalmol Vis Sci 1994; 35:3931-7.
4. Gonzalez-Fernandez F, Lopes MB, Garcia-Fernandez JM, Foster RG, De Grip WJ, Rosemberg S, Newman SA, VandenBerg SR. Expression of developmentally defined retinal phenotypes in the histogenesis of retinoblastoma. Am J Pathol 1992; 141:363-75.
5. Dyer MA, Bremner R. The search for the retinoblastoma cell of origin. Nat Rev Cancer 2005; 5:91-101.
6. Campbell M, Chader GJ. Retinoblastoma cells in tissue culture. Ophthalmic Paediatr Genet 1988; 9:171-99.
7. Schlesinger HR, Rorke L, Jamieson R, Hummeler K. Neuronal properties of neuroectodermal tumors in vitro. Cancer Res 1981; 41:2573-5.
8. Pardal R, Clarke MF, Morrison SJ. Applying the principles of stem-cell biology to cancer. Nat Rev Cancer 2003; 3:895-902.
9. Reya T, Morrison SJ, Clarke MF, Weissman IL. Stem cells, cancer, and cancer stem cells. Nature 2001; 414:105-11.
10. Bonnet D, Dick JE. Human acute myeloid leukemia is organized as a hierarchy that originates from a primitive hematopoietic cell. Nat Med 1997; 3:730-7.
11. Lapidot T, Sirard C, Vormoor J, Murdoch B, Hoang T, Caceres-Cortes J, Minden M, Paterson B, Caligiuri MA, Dick JE. A cell initiating human acute myeloid leukaemia after transplantation into SCID mice. Nature 1994; 367:645-8.
12. Al-Hajj M, Wicha MS, Benito-Hernandez A, Morrison SJ, Clarke MF. Prospective identification of tumorigenic breast cancer cells. Proc Natl Acad Sci U S A 2003; 100:3983-8. Erratum in: Proc Natl Acad Sci U S A 2003; 100:6890.
13. Singh SK, Clarke ID, Terasaki M, Bonn VE, Hawkins C, Squire J, Dirks PB. Identification of a cancer stem cell in human brain tumors. Cancer Res 2003; 63:5821-8.
14. Kondo T, Setoguchi T, Taga T. Persistence of a small subpopulation of cancer stem-like cells in the C6 glioma cell line. Proc Natl Acad Sci U S A 2004; 101:781-6.
15. Kim M, Turnquist H, Jackson J, Sgagias M, Yan Y, Gong M, Dean M, Sharp JG, Cowan K. The multidrug resistance transporter ABCG2 (breast cancer resistance protein 1) effluxes Hoechst 33342 and is overexpressed in hematopoietic stem cells. Clin Cancer Res 2002; 8:22-8.
16. Scharenberg CW, Harkey MA, Torok-Storb B. The ABCG2 transporter is an efficient Hoechst 33342 efflux pump and is preferentially expressed by immature human hematopoietic progenitors. Blood 2002; 99:507-12.
17. Zhou S, Schuetz JD, Bunting KD, Colapietro AM, Sampath J, Morris JJ, Lagutina I, Grosveld GC, Osawa M, Nakauchi H, Sorrentino BP. The ABC transporter Bcrp1/ABCG2 is expressed in a wide variety of stem cells and is a molecular determinant of the side-population phenotype. Nat Med 2001; 7:1028-34.
18. Doyle LA, Ross DD. Multidrug resistance mediated by the breast cancer resistance protein BCRP (ABCG2). Oncogene 2003; 22:7340-58.
19. Welm BE, Tepera SB, Venezia T, Graubert TA, Rosen JM, Goodell MA. Sca-1(pos) cells in the mouse mammary gland represent an enriched progenitor cell population. Dev Biol 2002; 245:42-56.
20. Summer R, Kotton DN, Sun X, Ma B, Fitzsimmons K, Fine A. Side population cells and Bcrp1 expression in lung. Am J Physiol Lung Cell Mol Physiol 2003; 285:L97-104.
21. Bhattacharya S, Jackson JD, Das AV, Thoreson WB, Kuszynski C, James J, Joshi S, Ahmad I. Direct identification and enrichment of retinal stem cells/progenitors by Hoechst dye efflux assay. Invest Ophthalmol Vis Sci 2003; 44:2764-73.
22. Goodell MA, Brose K, Paradis G, Conner AS, Mulligan RC. Isolation and functional properties of murine hematopoietic stem cells that are replicating in vivo. J Exp Med 1996; 183:1797-806.
23. Windle JJ, Albert DM, O'Brien JM, Marcus DM, Disteche CM, Bernards R, Mellon PL. Retinoblastoma in transgenic mice. Nature 1990; 343:665-9.
24. Reid TW, Albert DM, Rabson AS, Russell P, Craft J, Chu EW, Tralka TS, Wilcox JL. Characteristics of an established cell line of retinoblastoma. J Natl Cancer Inst 1974; 53:347-60.
25. Sery TW, Lee EY, Lee WH, Bookstein R, Wong V, Shields JA, Augsburger JJ, Donoso LA. Characteristics of two new retinoblastoma cell lines: WERI-Rb24 and WERI-Rb27. J Pediatr Ophthalmol Strabismus 1990; 27:212-7.

26. Alvi AJ, Clayton H, Joshi C, Enver T, Ashworth A, Vivanco MM, Dale TC, Smalley MJ. Functional and molecular characterisation of mammary side population cells. Breast Cancer Res 2003; 5:R1-8.
27. Goodell MA, McKinney-Freeman S, Camargo FD. Isolation and characterization of side population cells. Methods Mol Biol 2005; 290:343-52.
28. Seigel GM, Campbell LM. High-throughput microtiter assay for Hoechst 33342 dye uptake. Cytotechnology 2004; 45:155-60.
29. Russo JE, Hilton J. Characterization of cytosolic aldehyde dehydrogenase from cyclophosphamide resistant L1210 cells. Cancer Res 1988; 48:2963-8.
30. Armstrong L, Stojkovic M, Dimmick I, Ahmad S, Stojkovic P, Hole N, Lako M. Phenotypic characterization of murine primitive hematopoietic progenitor cells isolated on basis of aldehyde dehydrogenase activity. Stem Cells 2004; 22:1142-51.
31. Pellegrini G, Dellambra E, Golisano O, Martinelli E, Fantozzi I, Bondanza S, Ponzin D, McKeon F, De Luca M. p63 identifies keratinocyte stem cells. Proc Natl Acad Sci U S A 2001; 98:3156-61.
32. Maslov AY, Barone TA, Plunkett RJ, Pruitt SC. Neural stem cell detection, characterization, and age-related changes in the subventricular zone of mice. J Neurosci 2004; 24:1726-33.
33. Hashimoto K, Araki K, Osaki M, Nakamura H, Tomita K, Shimizu E, Ito H. MCM2 and Ki-67 expression in human lung adenocarcinoma: prognostic implications. Pathobiology 2004; 71:193-200.
34. Gallie BL, Dunn JM, Chan HS, Hamel PA, Phillips RA. The genetics of retinoblastoma. Relevance to the patient. Pediatr Clin North Am 1991; 38:299-315.
35. Abramson DH, Melson MR, Dunkel IJ, Frank CM. Third (fourth and fifth) nonocular tumors in survivors of retinoblastoma. Ophthalmology 2001; 108:1868-76.
36. Hemmati HD, Nakano I, Lazareff JA, Masterman-Smith M, Geschwind DH, Bronner-Fraser M, Kornblum HI. Cancerous stem cells can arise from pediatric brain tumors. Proc Natl Acad Sci U S A 2003; 100:15178-83.
37. Krishnakumar S, Mallikarjuna K, Desai N, Muthialu A, Venkatesan N, Sundaram A, Khetan V, Shanmugam MP. Multidrug resistant proteins: P-glycoprotein and lung resistance protein expression in retinoblastoma. Br J Ophthalmol 2004; 88:1521-6.

The print version of this article was created on 12 Sep 2005. This reflects all typographical corrections and errata to the article through that date. Details of any changes may be found in the online version of the article.